TRANSFORMATION OF MAGNETIC STATE UNDER THE INFLUENCE OF SUPERCONDUCTIVITY IN EPITAXIAL V/$Pd_{1-x}Fe_x$ BILAYERS

I.A. Garifullin[1], *N.N. Garif'yanov*[1], *D.A. Tikhonov*[1],
K. Theis-Bröhl[2], *K. Westerholt*[2], *and H. Zabel*[2]

[1] Zavoisky Physical-Technical Institute, Russian Academy of Sciences,
420029 Kazan, Russia
[2] Institut für Experimentalphysik/Festkörperphysik, Ruhr-Universität Bochum,
D-44780 Bochum, Germany

ИЗМЕНЕНИЕ МАГНИТНОГО СОСТОЯНИЯ В ЭПИТАКСИАЛЬНЫХ ДВУХСЛОЙНЫХ СИСТЕМАХ V/$Pd_{1-x}Fe_x$ ПОД ВОЗДЕЙСТВИЕМ СВЕРХПРОВОДИМОСТИ

И.А. Гарифуллин[1], *Н.Н. Гарифьянов*[1], *Д.А. Тихонов*[1], *М.З. Фаттахов*[1],
К. Чейс-Брёль[2], *К. Вестерхольт*[2], *Х. Цабель*[2]

[1] Физико-технический институт им. Завойского, Казань
[2] Университет Рура, Бохум, Bochum, Германия

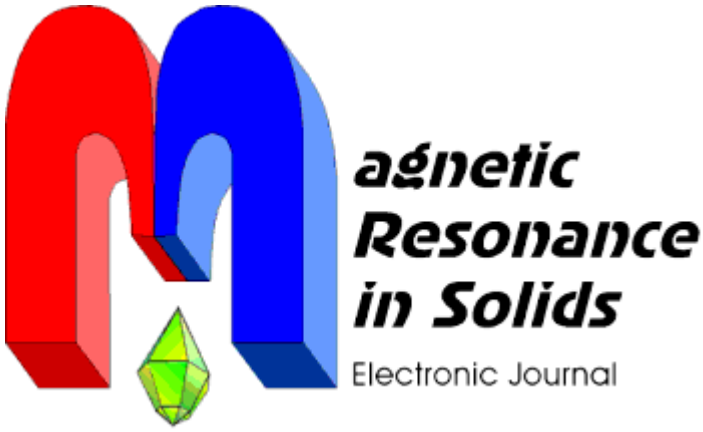

Volume **6**, *No.* **1**,
pages **51-58**, **2004**

http://mrsej.ksu.ru

TRANSFORMATION OF MAGNETIC STATE UNDER THE INFLUENCE OF SUPERCONDUCTIVITY IN EPITAXIAL V/$Pd_{1-x}Fe_x$ BILAYERS

I.A. Garifullin[1], N.N. Garif'yanov[1], D.A. Tikhonov[1],
K. Theis-Bröhl[2], K. Westerholt[2], and H. Zabel[2]
[1] *Zavoisky Physical-Technical Institute, Russian Academy of Sciences, 420029 Kazan, Russia*
[2] *Institut für Experimentalphysik/Festkörperphysik, Ruhr-Universität Bochum, D-44780 Bochum, Germany*

We have performed ferromagnetic resonance (FMR) studies of epitaxial V/$Pd_{1-x}Fe_x$ (001) bilayers with a V thickness of the order of 40 nm and with a $Pd_{1-x}Fe_x$ thickness in the range from 0.8 nm to 4.4 nm. For a bilayer with a $Pd_{1-x}Fe_x$ thickness of 1.2 nm and $x = 0.03$ the FMR measurements revealed a decrease of the effective magnetization $4\pi M_{\text{eff}}$ of the ferromagnetic layer below the superconducting transition temperature of vanadium. As a possible explanation for this decrease we suggest a spatial modulation of the ferromagnetic order in the $Pd_{1-x}Fe_x$ layer due to modifications of the indirect exchange interaction of magnetic ions via conduction electrons in the superconducting state. A comparison with a recent theoretical investigation supports this possibility.

1. Introduction

The destructive influence of ferromagnetism on superconductivity in dilute magnetic alloys and superconductor/ferromagnet (S/F) multilayers is well known (see, e.g., reviews [1] and [2-3], respectively). This occurs because the strong internal exchange field in the ferromagnetic state tends to align the conduction electron spins whose spin susceptibility $\chi_S(0)$ is zero in the superconducting state. Apart from the influence of ferromagnetism on superconductivity one can expect the realization of the S/F proximity in the opposite direction, i.e., a transformation of the ferromagnetic state under the influence of superconductivity. In order to understand the origin of this effect one has to go back to the roots i.e. to the early results on the electron spin resonance in a superconductor doped with magnetic impurities [4-6]. The authors of Refs. [4-6] found the long-range contribution to the Ruderman-Kittel-Kasuya-Yosida (RKKY) interaction between localized moments which arises upon transition to the superconducting state. This contribution has an antiferromagnetic origin and is caused by the superconducting correlations in the Cooper condensate. Much earlier Anderson and Suhl [7] proposed that the additional homogeneous polarization over a large distance from a magnetic impurity should appear in a superconductor. Theoretically the dependence of this polarization on the distance in a superconductor in a "clean" limit has been obtained in Refs. [6,8]. For a "dirty" limit Kochelaev *et al.* [9] showed that the homogeneous polarization of conduction electrons as well as the exchange interaction between the localized moments on the distance of the order of the superconducting coherence length (ζ_S) arises in a superconductor. It has the opposite sign relative to the homogeneous part of the polarization of conduction electrons induced by the exchange interaction between the localized moments and conduction electrons in a normal state. The polarization of conduction electrons in a superconductor with paramagnetic impurities integrated over the volume should vanish at T=0 K similarly to the situation for a superconductor without magnetic impurities. In spite of smallness of the "superconducting" polarization and the corresponding contribution to the RKKY interaction it should lead to the noticeable effects. In particular, this leads (see, e.g. [1]) to the helicoidal (or cryptoferromagnetic) magnetic ordering in some intermetallic compounds. As to a system consisting of a bulk superconductor with a thin ferromagnetic metallic film on its surface the possibility of the formation of a domain-like magnetic structure was considered theoretically by Buzdin and Bulaevskii [10]. They calculated the energy of two systems DS/S and F/S and concluded that the domain state (DS) will be the ground state for the magnetic layer thicknesses smaller than a certain critical thickness. The tendency for a reconstruction of the ferromagnetic order was observed experimentally in epitaxial Fe/Nb bilayers upon transition to the superconducting state [11]. This experimental result inspired further theoretical studies. Bergeret *et al.* [12] studied theoretically the possibility of a non-homogeneous magnetic order (cryptoferromagnetic state) due to superconductivity in heterostructures consisting of a bulk superconductor and a ferromagnetic thin layer. They derived a phase diagram which distinguishes the cryptoferromagnetic and ferromagnetic states and discussed the possibility of an experimental observation of the cryptoferromagnetic state in different materials. In particular, they concluded that because of the large magnetic stiffness constant and strong internal exchange field in pure iron the cryptoferromagnetic state is hardly possible in the Fe/Nb structure. Thus, it may be concluded that the tendency for a reconstruction of the ferromagnetic order in the iron layer observed experimentally in the Fe/Nb films [11], might be caused by discontinuous Fe layers in the thickness range where this effect was observed. Estimates performed by Bergeret *et al.* [12] show that the transition from the ferromagnetic to the cryptoferromagnetic state should be observable, if the exchange field and the magnetic stiffness constant would be an order of magnitude smaller than in pure Fe.

As a possible system for the experimental observation of the cryptoferromagnetic state in S/F multilayers the $V/Pd_{1-x}Fe_x$ system can be chosen because of its low (at $x < 0.1$) and tunable Curie temperature. Ferromagnetic resonance (FMR) measurements of bulk single crystals of $Pd_{1-x}Fe_x$ [13] suggest that these alloys are convenient systems for FMR studies because of their narrow resonance lines. In addition, it is well known (see, e.g., Ref. 14) that at any Fe concentration $Pd_{1-x}Fe_x$ alloys order ferromagnetically.

In this article we present our results on FMR measurements for $V/Pd_{1-x}Fe_x$ single crystalline epitaxial bilayers. We show an example where the saturation magnetization determined from the FMR spectra decreases with lowering the temperature below the superconducting transition temperature T_C.

The paper is organized as follows: in Section 2 we provide a brief outline of the sample preparation and their X-ray characterization. Then we describe the superconducting properties of the $V/Pd_{1-x}Fe_x$ bilayers as well as the electrical resistivity and the magnetization data. The FMR measurements are presented in Section 3, followed by a discussion of all the data in Section 4. The main results are summarized in Section 5.

2. Sample Preparation and Characterization

2.1. Sample Preparation

The $Pd_{1-x}Fe_x/V$ and $V/Pd_{1-x}Fe_x$ bilayers were grown on MgO (001) substrates in a molecular beam epitaxy system (base pressure ~ $5 \cdot 10^{-11}$ mbar). During the evaporation the background pressure was below 10^{-9} mbar. The MgO (001) substrates were annealed in the growth chamber at 1000 ^oC for 0.5 h prior to the evaporation in order to desorb impurities and to create a well ordered surface. Then the substrates were cooled to the desired temperature.

For the $Pd_{1-x}Fe_x/V/MgO$ (001) samples (samples 1-4 in Table I) the substrate temperature during the evaporation of the first V layer was 550^o C. The evaporation rates of 0.01 nm/s were found to be optimal for the growth of high quality single crystalline V (001) films. $Pd_{1-x}Fe_x$ (001) films were prepared using two sources. Fe was evaporated from

an effusion cell providing a flux of high stability, while Pd was evaporated by an electron beam gun. The substrate temperature during the preparation of the $Pd_{1-x}Fe_x$ layer was 200°C. The deposition rate of Pd was 0.027 nm/s and the Fe deposition rate varied between 0.0027 nm/s and 0.0009 nm/s.

For the V/$Pd_{1-x}Fe_x$/Pd/MgO (001) samples (samples 5 and 6) a buffer Pd (001) layer of about 100 nm was grown on MgO. The substrate temperature during the preparation of the Pd buffer layer was 450° C for the sample 5, and 400° C for the sample 6. The substrate temperature during the evaporation of the $Pd_{1-x}Fe_x$ (001) layer was 450° C and 400° C for the samples 5 and 6, respectively. The V layer was deposited using a substrate temperature of 300° C and the evaporation rate given above. In both cases the bilayers (except the sample 1) were covered by a protective layer of Pd with a thickness of a few nanometers. The substrate temperature during the growth of the protective layer was 200° C.

Table I. *Experimental parameters of the studied samples*

Sample	d_V (nm)	d_{Pd} + d_{PdFe} (nm) (X-ray)	T_{Curie} (K)	d_{PdFe} (nm) (SQUID)	*RRR*	T_C (K)	$4\pi M_{eff}(30K)$ (kG)	K_1/M (Oe)
1	37.2	4.4	250	4.4	4.7	4.0	3.9	15.8
2	40.0	6.2	100	1.2	5.0	4.2	2.6	65.0
3	39.3	6.2	100	3.0	4.0	3.8	1.7	80.0
4	47	6.8	90	0.8	4.6	4.0	-	-
5	41.0	103	120	0.9	4.0	3.7	-	-
6	37.0	101	100	1.0	4.5	3.1	1.8	72.0

Given are the thickness of the V layer d_V and of the Pd and $Pd_{1-x}Fe_x$ layers $d_{Pd}+d_{PdFe}$ obtained from the fit of the small angle reflectivity scans, the Curie temperature T_{Curie} and the thickness of the magnetic $Pd_{1-x}Fe_x$ layer obtained from the SQUID magnetization measurements, residual resistivity ratio *RRR*, the superconducting transition temperature T_C, $4\pi M_{eff}$ and K_1/M values obtained from FMR measurements.

The growth rates were measured by a quartz-crystal monitor. The final thickness of the $Pd_{1-x}Fe_x$ layer was determined by the evaporation time. The quality of the substrate and of each layer was always controlled by in-situ RHEED characterization to ensure a high quality growth of our samples. Each sample was prepared separately, but with identical growth conditions. The sample holder was rotated during the deposition to ensure a homogeneous film thickness.

Six samples with the experimental parameters summarized in Table I have been investigated by FMR.

2.2. X-ray Characterization

The intensity of specularly reflected X-rays at small angles provides information on the average electron density profile of the material studied in the direction along the surface normal. X-ray reflectivity measurements were performed *ex situ* using a 1.5 kW X-ray generator with a Mo anode (λ = 0.709 nm) and a Si (111) monochromator. The reflectivity scans showed well resolved oscillations. Fits of these scans gave an interface roughness of less than 4 Å, indicating the high interfacial quality of our samples. The film thicknesses, as obtained from the fits to the X-ray data are given in Table I. The thicknesses d_{Pd} of the top Pd layer in the case of Pd/$Pd_{1-x}Fe_x$/V/MgO samples and of the Pd buffer layer in case of V/$Pd_{1-x}Fe_x$/Pd/MgO samples are shown in Table I together with $d_{Pd\text{-}Fe}$ as $d_{Pd}+d_{Pd\text{-}Fe}$.

A typical radial Bragg scans covering the angle range of the V (002) and $Pd_{1-x}Fe_x$ (002) peaks for the sample 2 with d_V = 40 nm and $d_{Pd} + d_{Pd\text{-}Fe}$ = 6.2 nm reveal the (001) texture of both, the V layer and $Pd_{1-x}Fe_x$ layer.

2.3. Superconducting Transition Temperature

The superconducting transition temperature T_C was measured resistively using a standard four-terminal configuration with the current and voltage leads attached to the samples with the silver paint. T_C was defined as the midpoint of the superconducting transition. The T_C values are presented in Table I. For all samples the superconducting transition was very sharp with a transition width of the order of 0.1 K.

2.4. Electrical Resistivity

The residual resistivity ratio $RRR = R(300\text{ K})/R(T_C)$ for the samples listed in Table I varies between 4 and 5. The corresponding residual resistivity values (from 4.6 to 6.1 μΩ·cm) allow to estimate the electron mean-free path l_S for V using the Pippard relations [15]

$$\sigma = e^2 S < l_S > /12\pi^3\hbar \quad \gamma = k_B^2 S/12\pi\hbar < v_F > \tag{1}$$

where σ denotes the electrical conductivity, γ the electronic specific heat coefficient, v_F the Fermi velocity of the conduction electrons, and l_S the mean-free path of conduction electrons. *S* is the Fermi surface area and the brackets indicate a mean average over the Fermi surface. Combining relations (1), one obtains

$$\rho l_S = (\pi k_B / e)^2 = (1 / v_F \gamma). \tag{2}$$

This relation permits an estimate of l_S from the low temperature resistivity ρ and the coefficient of the electronic specific heat γ. For V using $\gamma = 9$ mJ/mole K^2 and $v_F = 3 \cdot 10^7$ cm/s [16], we find $\rho l_S = 2.46 \cdot 10^{-6}$ $\mu\Omega$cm^2. This gives l_S-values between 4 and 5 nm.

2.5. Magnetization

Magnetization measurements using a SQUID magnetometer were performed with the film surface parallel to the direction of the magnetic field. For the precise determination of the ferromagnetic magnetization the correction of the substrate contribution to the magnetic moment of the samples is very important. The measurements of the temperature dependence of the magnetization of the MgO substrates used in the present study showed that at temperatures below 4 K the magnetic susceptibility of the substrates starts to increase strongly.

The measurements of the temperature dependence of the magnetization have been performed at a small magnetic field H = 10 Oe for all samples. The temperature dependencies of the magnetization in the ferromagnetic state after subtraction the substrate contribution are shown in Fig. 1 for two samples. They are typical for bulk $Pd_{1-x}Fe_x$ alloys (see, e.g., Ref. 17) The values obtained for the ferromagnetic Curie temperature T_{Curie} are presented in Table I. These values of T_{Curie} allows us to estimate the Fe concentration in $Pd_{1-x}Fe_x$ alloy layers of our samples using the data for $T_{Curie} = f(x)$ from the review by Nieuwehuys [14]. Values of x determined in such a way lie between 0.03 and 0.1. Magnetization values corresponding to these concentrations, give the ferromagnetic layer thickness $d_{Pd\text{-}Fe}$ from our SQUID magnetization data. These values are also shown in Table I. The difference observed between the film thicknesses determined by X-rays and the magnetization measurements are due to the fact that for X-rays there is basically no electron density contrast between Pd and $Pd_{1-x}Fe_x$. Therefore with X-ray reflectivity measurements the sum of both layer thicknesses is determined.

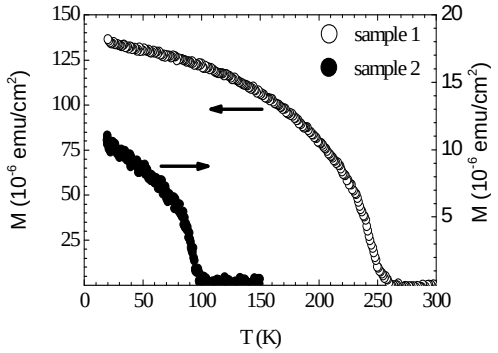

Fig. 1. Saturation magnetization per unit surface for the samples 1 and 2 vs temperature measured by SQUID magnetometer in the magnetic field H = 10 Oe parallel to the film plane

3. FMR Results and Analysis

Ferromagnetic resonance (FMR) experiments were carried out at 9.4 GHz in the temperature range from 1.6 K to 250 K using the ESR spectrometer B-ER 418^S (Bruker AG). In the normal state of the samples (T > 4.2 K) the FMR signals were observed for four of our samples: 1, 2, 3 and 6; for other two samples the resonance lines were not found. The angular dependence of the spectra was studied in the in-plane geometry, i.e. with both the dc magnetic field and the high frequency field lying in the film plane. The (001) surface of our thin films contains two principal magnetic axes of the bulk $Pd_{1-x}Fe_x$ crystal ([100] and [110] axes). The observed angular dependence of the resonance exhibits a four-fold anisotropy typical for cubic crystals in the (001)-plane. As an example the angular dependence of the resonance field H_0 of the FMR signal for the samples 1 and 2 is shown in Fig. 2.

A qualitatively similar behavior of H_0 was observed for the samples 3 and 6 as well. One can see from Fig. 2 that the [110] axis is the magnetically easy axis for our samples. In the superconducting state we were able to study the behavior of the FMR line parameters for the samples 1 and 2 only. This is due to a drastic increase of the intensity of the electron paramagnetic resonance of non-controlled paramagnetic impurities in the MgO substrate at temperatures below 4 K. This background prevented the observation of the FMR signal from $Pd_{1-x}Fe_x$ layers for the samples 3 and 6 in the superconducting state. Examples of FMR lines of the sample 2 in the normal and superconducting state after subtraction of the background signal are shown in Fig. 3 for the dc magnetic field along the magnetically easy axis.

The FMR results are analyzed using a coordinate system in which the magnetization **M** of the $Pd_{1-x}Fe_x$ layer makes an angle θ with respect to the film normal (z direction) and an angle φ with respect to the x axis in the film plane (xy plane). The external magnetic field H is applied at an angle θ_H with respect to the film normal and at an angle φ_H with respect to the x axis. We define the x axis to be parallel to the [100] axis of the $Pd_{1-x}Fe_x$ layer. In our experiments θ_H was equal to $\pi/2$.

In general, thin films of materials with a cubic structure grown along the [001] crystallographic axis have a tetragonal symmetry as a result of the in-plane strain due to epitaxial mismatch. This leads to

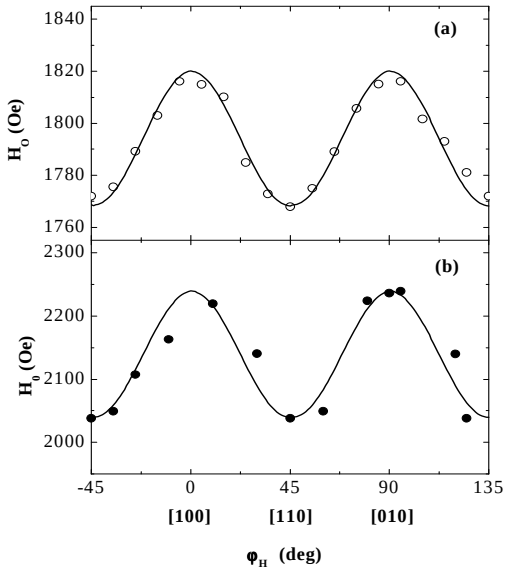

Fig. 2. In-plane angular dependencies of the resonance field H_0 for the sample 1 (a) and the sample 2 (b) at T = 30 K. The solid lines are the calculated resonance field values with parameters: K_1/M = 15.8 Oe, $4\pi M_{eff}$ = 3.9 kG (for the sample 1) and K_1/M = 65 Oe, $4\pi M_{eff}$ = 2.6 kG (for the sample 2)

the corresponding out-of plane Poisson distortion. Therefore, the contribution to the free energy due to the crystal anisotropy should contain the four-fold in-plane anisotropy constants, which differ from the fourth-order constant for the direction perpendicular to the film plane. In addition, a non-zero second-order uniaxial anisotropy term appears, due to the vertical lattice distortion and the broken symmetry of the crystal field acting on the interface atomic layer. The corresponding energy term has the form $F_u = -K_u \cos^2 \vartheta$. Since our experiments were performed in the in-plane geometry only, we will use the crystal anisotropy energy for cubic instead of tetragonal symmetry. Uniaxial perpendicular anisotropy and the contribution of the dipolar interaction (demagnetizing field $4\pi M$) enter the free energy of a system in an additive way, and therefore one can introduce an effective demagnetizing field

$$4\pi M_{eff} = 4\pi M - \frac{2K_u}{M}, \qquad (3)$$

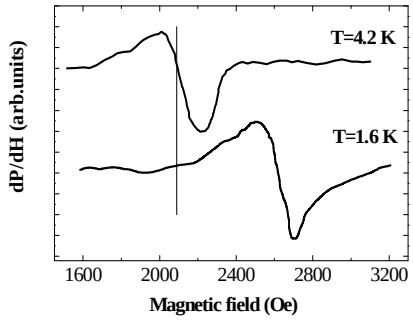

Fig. 3. FMR spectra for the sample 2 at T = 4.2 K (normal state) and 1.6 K (superconducting state) with dc magnetic field along the [110] axis of the Pd$_{1-x}$Fe$_x$ layer

in order to account for the second-order perpendicular uniaxial anisotropy. Thus the total magnetic free energy density function appropriate for a (001)-oriented film is written in the form:

$$F = -MH \sin\vartheta\cos(\varphi - \varphi_H) + 2\pi M_{eff}^2 \cos^2\vartheta + \frac{1}{4}K_1(\sin^2 2\vartheta + \sin^4\vartheta\sin^2\varphi). \qquad (4)$$

Here K_1 is the fourth-order cubic anisotropy constant.

The equilibrium position of **M** is given by the zeros of the first angle derivatives of F. In our experimental situation the out-of plane equilibrium angle is $\vartheta_0 = \pi/2$, and the in-plane equilibrium angle φ_0 is given by the solution of equation

$$H\sin(\varphi_0 - \varphi_H) = -\frac{K_1}{2M}\sin(4\varphi_0). \qquad (5)$$

Using the general ferromagnetic resonance condition [19]

$$\left(\frac{\omega}{\gamma_0}\right)^2 = \frac{1}{(M\sin\theta)^2}\left[\frac{\partial^2 F}{\partial\vartheta^2}\frac{\partial^2 F}{\partial\varphi^2} - \left(\frac{\partial^2 F}{\partial\vartheta\partial\varphi}\right)^2\right], \qquad (6)$$

we obtain:

$$\left(\frac{\omega}{\gamma_0}\right)^2 = \left[H\cos(\varphi_0 - \varphi_H) + \frac{2K_1}{M}\cos(4\varphi_0)\right]\times$$
$$\times\left[H\cos(\varphi_0 - \varphi_H) + 4\pi M_{eff} + \frac{K_1}{2M}(3 + \cos(4\varphi_0)\right]. \qquad (7)$$

Here $\gamma_0 = g\mu_B/\hbar$ and g is the spectroscopic g-value. The expression (7) together with the condition for equilibrium (5) determines the resonance field position H_0 as a function of the angle φ_H, of the effective magnetization $4\pi M_{\text{eff}}$, and of the anisotropy constant K_1.

We analyzed numerically the influence of all parameters in Eqs. (5) and (7) on the angular dependencies of the resonance field and obtained the following features: The increase of the $4\pi M_{\text{eff}}$ value leads to a total shift of the resonance field to lower values. The increase of K_1/M leads to an increase of the amplitude of variation of $H_0(\varphi_H)$.

To fit the angular dependencies of the resonance field $H_0(\varphi_H)$, we used Eqs. (5) and (7). Typical results with g = 2.09 are shown in Fig. 2. They are in a good agreement with our experimental data. These fits gave us K_1 and $4\pi M_{\text{eff}}$ values.

In order to determine the temperature dependence $4\pi M_{\text{eff}}(T)$, we used the temperature dependence of the resonance field measured with the dc magnetic field along the magnetically easy [110] axis of the Pd$_{1-x}$Fe$_x$ layer. Using Eqs. (5) and (7) at $\varphi_H = \pi/4$ from the temperature dependence of H_0, we obtain the temperature dependencies of $4\pi M_{\text{eff}}$ for the samples 1 and 2 in a wide temperature range as shown in Fig. 4.

Our study of the resonance field at fixed φ_H -value for the sample 2 clearly reveals a shift of the resonance field to higher values when decreasing the temperature below the superconducting transition temperature T_C (see Fig. 3). The latter fact definitely shows that the observed temperature dependence of H_0 at an orientation of the dc magnetic field along easy axis is caused by a decrease of the effective

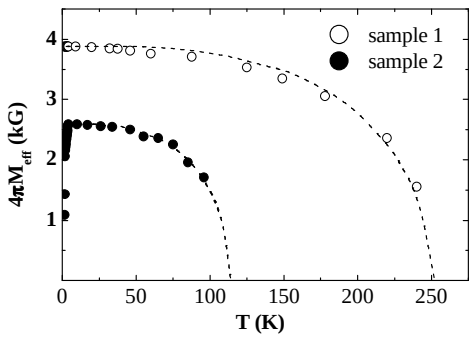

Fig. 4. $4\pi M_{eff}$ vs temperature for the samples 1 and 2 as revealed by FMR measurements. Dashed lines are the theoretical curves for S = 1/2 from the molecular field theory

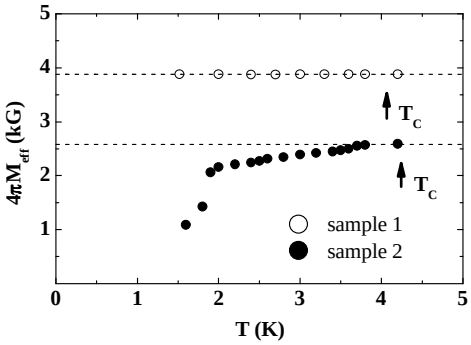

Fig. 5 Low temperature parts of $4\pi M_{\text{eff}}$ for the samples 1 and 2. The arrows show the T_C values at the resonance field H_0

magnetization $4\pi M_{\text{eff}}$. The low temperature part of $4\pi M_{\text{eff}}(T)$ derived from that of H_0 is shown in Fig. 5. For comparison we also show the data obtained for the sample 1, where such behavior is not observed. Here we use the low temperature values of K_1/M and assume that they do not change noticeably in the temperature range from 10 K to 1.6 K.

4. Discussion

The most interesting result of the present study is the decrease of the effective magnetization $4\pi M_{\text{eff}}$ below the superconducting transition for the sample 2 (Fig. 5). At the same time $4\pi M_{\text{eff}}$ for the sample 1 does not change in this temperature region. In accordance with expression (3), a decrease of $4\pi M_{\text{eff}}$ can be caused by a decrease of the saturation magnetization M or by an increase of the perpendicular uniaxial anisotropy constant K_u. One can expect that the uniaxial anisotropy, which appears usually due to the broken symmetry of crystal field acting on the interface atomic layer, is proportional to the reciprocal thickness of the ferromagnetic layer. Comparison of the values of $4\pi M_{\text{eff}}$ for the samples 3 and 6 with nearly the same Fe content (according to the same values of T_{Curie}) but different thicknesses indicates that the second-order perpendicular uniaxial anisotropy is negligible in the thickness range studied here. Thus we have to conclude that the decrease of $4\pi M_{\text{eff}}$ is caused by a decrease of the saturation magnetization M.

We believe that a decrease of the saturation magnetization below T_C , which is observed for the sample 2, is caused by a transformation of the homogeneous ferromagnetic order in the $Pd_{1-x}Fe_x$ magnetic layer due to the proximity effect with the superconducting layer. It is well known (see, e.g., [2]) that the superconducting order parameter is strongly suppressed near the S/F interface. This is due to a penetration of the Cooper pairs into the ferromagnet where they are subjected to the strong exchange field. This leads to a T_C-suppression. The destructive influence of the exchange field on the superconductivity can considerably be weakened, if a domain structure on a length scale smaller than the superconducting coherence length ξ_S appears in the ferromagnetic layer, because then the exchange field would be effectively cancelled over the dimension of the Cooper pairs [7]. As it was mentioned in Introduction, a possible non-homogeneous magnetic order in a system consisting of a bulk superconductor with a thin ferromagnetic metallic film on its surface was considered by Buzdin and Bulaevskii [10] for the first time. They obtained that the domain state will be the ground state for a magnetic layer thickness

$$d_M^{crit} \le \left(\frac{T_C^2}{T_{Curie} h} l_S \xi_0^{1/2} \right)^{2/3} \tag{8}$$

where h is the exchange field acting on the conduction electrons in the ferromagnetic layer and ξ_0 is the superconducting coherence length of the pure material ($\xi_S = 0.85\sqrt{\xi_0 l_S}$). For the sample 2 we have $T_C = 4.2$ K, $T_{\text{Curie}} = 100$ K, $l_S \sim 5$ nm, and $\xi_0 = 70$ nm. From the Curie temperature we estimate the Fe concentration in the $Pd_{1-x}Fe_x$ layer as 3 at.% in accordance with Ref. 14. This gives $h \sim 100$ K and $d_M^{crit} \sim 0.2$ nm. Since for our sample $d_{\text{Pd-Fe}} = 1.2$ nm, this estimate suggests that in our case the decrease of the magnetization cannot be due to cryptoferromagnetism. On the other hand, recently Bergeret *et al.* [12] criticized the assumptions taken in Ref. 10 and concluded that these results can hardly be used for quantitative estimates. They presented a microscopic derivation of the phase diagram valid for realistic parameters of the problem involved. They considered a cryptoferromagnetic state i.e. a state in which a magnetic moment rotates in space and concluded that in the absence of a strong anisotropy this state is more favorable than the domain structure of Ref. 10. Bergeret *et al.* [12] determined the phase diagram in the vicinity of the superconducting transition for two variables:

$$a = \frac{h d_M}{\eta} \sqrt{\frac{2}{D_S T_C}} \ , \tag{9}$$

which takes into account the exchange splitting h of conduction band in a ferromagnet and

$$\lambda = \frac{J d_M}{\gamma \sqrt{2 T_C D_S^3}} \frac{7\xi(3)}{2\pi^2} \tag{10}$$

accounting for the magnetic stiffness J of the ferromagnetic layer. Here $\eta = v_{FM}/v_{FS}$ is the ratio of the Fermi velocities of the ferromagnet v_{FM} and superconductor v_{FS}, D_S is the diffusion coefficient in the superconductor and γ is the electronic density of states for a superconductor. The obtained phase diagram is represented in Fig. 2 of Ref. 12. The curves are plotted for different values of $\tau = (T_C - T)/T_C$.

In the following we make an estimate for our samples according to the phase diagram of Bergeret *et al.* [12]. The magnetic stiffness J is roughly proportional to the Curie temperature. For Fe with $T_{\text{Curie}} \sim 1000$ K it is of the order of 600 K/nm. So, for our sample 2 with $T_{\text{Curie}} \sim 100$ K it should be 60 K/nm. As we supposed above, the exchange splitting of the conduction band of ferromagnetic $Pd_{0.97}Fe_{0.03}$ is $h \sim 100$ K, the Fermi velocity $v_{FS} = 3 \cdot 10^7$ cm/s corresponds to the diffusion coefficient $D_S \sim 5$ cm^2/s. Assuming that the Fermi velocities of conduction electrons in V and $Pd_{1-x}Fe_x$ are close to each other we obtain $a \sim 1.2$ and $\lambda \sim 1.3 \cdot 10^{-3}$ for our sample 2. In accordance to the phase diagram by Bergeret *et al.*[12] this implies that

starting from $\tau \sim 0.2$ ($T \sim 3$ K) a transition from the ferromagnetic to the cryptoferromagnetic state should take place. Actually this transition is observed experimentally at $T \sim 2$ K which is close to the expected transition point. For the sample 1 with d_M~4.4 nm and T_{Curie}~250 K we have a~20 and $\lambda \sim 1.4 \cdot 10^{-2}$. With these values of parameters the ferromagnetic state is stable at any temperatures, as it is observed experimentally. Thus, these estimates support the conclusion concerning the observation of a phase transition from the ferromagnetic to the cryptoferromagnetic state in our sample 2.

5. Summary

In summary, FMR measurements of V/$Pd_{1-x}Fe_x$ bilayers prepared by molecular beam epitaxy have been performed over a wide temperature range. We find a decrease of the saturation magnetization of the $Pd_{1-x}Fe_x$ magnetic layer below the superconducting transition temperature for the V/$Pd_{1-x}Fe_x$ bilayer system with $x \sim 0.03$ and $d_{Pd\text{-}Fe} = 1.2$ nm. We regard this as a clear indication of the formation of the non-homogeneous cryptoferromagnetic state in the $Pd_{1-x}Fe_x$ layer due to S/F proximity effect.

Acknowledgements

The authors would like to thank Dr. S.Ya. Khlebnikov (Kazan) for his assistance in the low temperature measurements and J. Podschwadek (Bochum) for assistance in the sample preparation. This work is supported by the Deutsche Forschungsgemeinschaft (SFB 491) and by the Russian Fund for Basic Research (Project No. 02-02-16688).

References

1. Buzdin A.I., Bulaevskii L.N., Kulic M.L., Panyukov S.V. *Adv. Phys.* **34**, 175 (1985).
2. Garifullin I.A. *J. Magn. Magn. Mater.* **240**, 574 (2002).
3. Izyumov Yu.A., Proshin Yu.N., Khusainov M.G. *Physics – Uspekhi* **45**, 109 (2002).
4. Alekseevskii N.E., Garifullin I.A., Kochelaev B.I., and Kharakhash'yan E.G. *JETP Lett.* **18**, 189 (1973).
5. Kochelaev B.I., Kharakhash'yan E.G., Garifullin I.A., and Alekseevskii N.E. *Proceedings of the Eighteenth Congress AMPERE, Nottingham, 1974*, p.23 (1974) (invited).
6. Alekseevskii N.E., Garifullin I.A., Kochelaev B.I., and Kharakhash'yan E.G. *Sov.Phys. JETP*, **45**, 799 (1977).
7. Anderson P.W., Suhl H. *Phys.Rev.*, **116**, 898 (1959).
8. Hurault J.P. *J.de Phys.* **26**, 252 (1965).
9. Kochelaev B.I., Tagirov L.R., and Khusainov M.G. *Sov.Phys. JETP* **49**, 291 (1979).
10. Buzdin A.I., Bulaevskii L.N. *Sov. Phys. JETP* **67**, 576 (1988).
11. Mühge Th., Garif'yanov N.N., Goryunov Yu.V., Theis-Bröhl K., Westerholt K., Garifullin I.A., Zabel H. *Physica* C **296**, 325 (1998).
12. Bergeret F.S., Efetov K.B., Larkin A.I. *Phys. Rev.* B **62**, 11872 (2000).
13. Bagguley D.M.S., and Robertson J.A. *J. Phys.*F **4**, 2282 (1974).
14. Nieuwehuys G.J. *Adv.Phys.* **24**, 515 (1975).
15. Pippard A.B. *Rep. Prog. Phys.* **23**, 176 (1960).
16. Gschneider K.A. *Solid State Phys.* **16**, 275 (1964).
17. Crangle J. *Phil. Mag.* **5**, 335 (1960).
18. Suhl H. *Phys. Rev.* **97**, 555 (1955).